Liquid-Phase Composition of Intact Fruit Tissue Measured by High-Resolution Proton NMR

Qing Wen Ni and Thomas M. Eads*

Department of Food Science and Whistler Center for Carbohydrate Research, 1160 Smith Hall, Purdue University, West Lafayette, Indiana 47906-1160

High-resolution ^1H (proton) NMR spectra were obtained on intact fruit tissues (grape, banana, and apple). Liquid-phase component line widths showed field-dependent broadening due to magnetic susceptibility effects; the effect was larger in more physically heterogeneous tissues (apple > banana > grape). Magic angle spinning (MAS) reduced susceptibility broadening, while water peak suppression increased dynamic range, enabling detection of components at levels at least as low as 0.01% of fresh weight. Water, glucose, fructose, sucrose, organic acids (malic, citric, tartaric), and total fatty acyl lipids were quantified. Longitudinal relaxation times of nonexchangeable glucose protons were measured *in situ* in banana and found to be dominated by intra- and intermolecular homonuclear dipolar interactions. This is similar to the situation *in vitro*. Apparently, rotational motions of the water and sugar molecules within the fruit are relatively unhindered. The combined results have implications for nondestructive analysis of heterogeneous materials and for design of new devices for quality assessment, laboratory analysis, and process monitoring.

INTRODUCTION

The methods of nuclear magnetic resonance (NMR) provide nondestructive approaches for quantifying the chemical and physical properties of agricultural materials related to their quality. Detection of specific components by NMR requires observation of individual signals from them. Specific signals from the liquid phase of heterogeneous materials can be detected as resonances in an NMR spectrum, as in high-resolution pulse Fourier transform NMR (Coombe and Jones, 1983; Eads and Bryant, 1986; Cho et al., 1991; Rutar et al., 1988; Bellon et al., 1992; Ni and Eads, 1992a), or as components of the induction signal, as in pulse time domain NMR (Tellier et al., 1989). The selectivity is greatest in high-resolution NMR, but new relaxation methods show promise in applications requiring detection of one or a few analytes other than water (Guillou and Tellier, 1988). The practical significance of the high-resolution technique for fruit was illustrated recently by nondestructive measurement of total sugar content by ^1H NMR (Cho and Krutz, 1989; Cho et al., 1991) and of sugar composition and molecular mobility by ^{13}C NMR (Ni and Eads, 1992a) in samples of intact fruit tissue. Nonetheless, the limits of sensitivity and selectivity for nondestructive chemical analysis of heterogeneous materials by multinuclear high-resolution NMR remain largely unexplored.

When high-resolution proton NMR was previously used in an attempt to measure sugar content in fruit tissue (Cho et al., 1991), only a broad envelope containing sugar proton resonances was observable and individual sugars could not be observed. The lack of resolution was ascribed to susceptibility broadening. This effect is characteristic of physically inhomogeneous materials. It has been shown in previous studies that low-speed magic angle spinning (MAS at a few hundred hertz) simultaneously relieves susceptibility broadening, improves resolution, produces accurate chemical shifts, and increases signal-to-noise ratio (S/N) (Doskocilova et al., 1975; Rutar et al., 1988; Eads, 1991; Eads et al., 1991; Ni and Eads, 1992a; Longo et al., 1992). Realization of these advantages for fruit tissue observed by ^{13}C NMR led to measurement of sugar composition and molecular rotational correlation times (Ni and Eads, 1992a). However, with the particular ^{13}C method used, it took at least an hour to obtain adequate S/N and minor components were not visible. As we show here, acquiring the corresponding MAS ^1H NMR spectrum only takes tens of seconds, due to the inherently higher sensitivity of this nucleus. However, in fresh fruit, the water proton resonance intensity is very strong, and so water peak suppression is necessary.

Low-speed MAS and water peak suppression are shown to greatly improve resolution and dynamic range for detection of liquid-phase components at levels at least as low as 0.01% in fresh fruit, in the presence of intense resonances from more abundant component dynamic range. Resonances can be assigned, and composition can be obtained by integration. ^1H nuclear relaxation results are shown to give additional insight into molecular mobility of components and into the origins of residual line broadening in MAS spectra.

EXPERIMENTAL PROCEDURES

Sample Preparation. As previously described (Ni and Eads, 1992a), a cylindrically shaped piece of edible fruit tissue was cut and transferred to an NMR tube for the conventional high-resolution probe or to a rotor for the MAS probe.

NMR Methods. Most ^1H NMR spectra were acquired on a high-resolution NMR spectrometer (Nicolet NT 200), with a 4.7-T superconducting solenoid magnet. The spectrometer was upgraded with a TecMag Libra interface (TecMag, Houston, TX) and Apple Macintosh IIfx computer data system running TecMag MacNMR data acquisition and processing software. For MAS experiments the rotor axis makes an angle of 54° 44′, the "magic angle", with the static applied field. Other details were given previously (Ni and Eads, 1992a). This spectrometer has an operating frequency of 200.067 MHz for ^1H. A two-channel probe equipped for magic angle spinning (Doty Scientific, Inc., Columbia, SC) was used, but for proton MAS experiments, the high-frequency channel was used for both ^1H excitation and detection. Sample temperature was maintained at 22 ± 1 °C. Conventional (non-MAS) spectra were also obtained on instruments at Purdue University operating at ^1H frequencies of 300,

* Author to whom correspondence should be addressed [telephone (317) 494-1749; fax (317) 494-7953].

0021-8561/93/1441-1026$04.00/0

500, and 600 MHz, and the 60-MHz non-MAS spectrum was obtained on a Hitachi–Perkin-Elmer R-24B spectrometer at Great Lakes Chemical Corp., West Lafayette, IN.

For single-pulse experiments the following pulse sequence was used: $(D_0\text{–}P_1\text{–acquisition})_n$, where D_0 is a delay of about 15 s, which is 10 times longer than the longest ^1H longitudinal relaxation time (T_1) in the fruits observed [$T_1(^1H_2O) = 1.4$ s]. P_1 is the radio frequency excitation pulse, set to 5 μs to produce a 90° tip angle in the MAS probe on a standard sample (10% D_2O, 90% H_2O) and 11 μs (90°) for the conventional probe. The 5-μs value for P_1 was suitable for homogeneous samples such as glucose in water. For fresh banana tissue, however, the effective 90° pulse was 14 μs in the MAS probe. In most spectra, only four scans were accumulated using quadrature phase cycling. Typical sweep width was 2 kHz, with a data size of 4096 points. Typical acquisition times were 1.02 s. Free induction decays (FIDs) were multiplied by an exponential function (line broadening of 1 Hz) to improve signal-to-noise ratio and, when needed, by a combined Gaussian–exponential multiplication to enhance resolution (Figure 5).

Spectral acquisition parameters were usually adjusted to optimize the signal-to-noise ratio of the weakest resonances. In cases where the water signal was very intense, preamplified signal must be attenuated to prevent ADC overflow ("clipping"), with concomitant reduction in sensitivity for detection of minor components (compare spectra A and B of Figure 3). For water peak suppression by presaturation, the pulse sequence was $(D_0\text{–}P_2\text{–}P_1\text{–acquisition})_n$, where the presaturation pulse P_2 was applied exactly at the water resonance frequency. On the NT200, this was accomplished using the decoupler channel in heteronuclear mode. The presaturation pulse duration was 400 ms, and the radio frequency (rf) field strength was 400 Hz (proton precession frequency).

To optimize sample condition during NMR measurements, the minimum spinning rates should be used, as described by Ni and Eads (1992a). In the spectra reported here, MAS rates were 300–1000 Hz.

Longitudinal relaxation (T_1) measurements were made by the inversion–recovery Fourier transform (IRFT) method (Vold et al., 1968). The IRFT sequence is $(D_0\text{–}180°\text{–}\tau\text{–}90°\text{–acquisition})$, where τ is the variable delay. Nine values of τ ranging from 1 ms to 10 s were used to acquire a T_1 data set. Data were analyzed by fitting individual peak heights $M(\tau)$ from the spectra to

$$M(\tau) = M_0[1 - 2(\exp(-\tau/T_1))] \quad (1)$$

T_1 of fructose was obtained from analysis of the peak at 3.89 ppm containing overlapping resonances of fructose and sucrose by fitting to

$$M(\tau) = M_{0,\text{suc}}[1 - 2(\exp(-\tau/T_{1\text{suc}}))] + M_{0,\text{fruc}}[1 - 2(\exp(-\tau/T_{1\text{fruc}}))] \quad (2)$$

where $M_{0,\text{suc}}$ and $M_{0,\text{fruc}}$ are the equilibrium magnetization values for sucrose and fructose; $T_{1\text{suc}}$, the relaxation time for sucrose, was obtained from analysis of the unique sucrose H-3′ resonance at 4.10 ppm in the same spectrum. The remaining constants were obtained by fitting.

Integration of Spectra and Calculation of Composition. From single-pulse MAS spectra obtained without water peak suppression, the integrals of water and sugar were obtained. From spectra acquired with water peak suppression, the sugar, lipid, and acid integrals were obtained. The lipid and acid integrals were calibrated by the ratio of sugar integrals from the two experiments. Some peaks contain resonance intensity from more than one component. In those cases, correction was made to the total integrals for each component as follows. The peak at 2.50–2.84 ppm contains resonances from methylene protons at positions between double bonds in polyunsaturated fatty acyl chains of lipids, plus resonances from nonexchangeable protons of malic acid and citric acid. The peak centered at 5.30 ppm contains resonances from CH protons at positions of unsaturation in fatty acyl chains of lipids, plus the sucrose H-1 proton (i.e., the anomeric proton of glucosyl residue). The total lipid integral was calculated as

$$\sum_\delta I_{\text{lipid},\delta} = I_{(0.66\text{–}2.50\text{ ppm})}[1 + (0.019 + 0.038)f] \quad (3a)$$

where 0.019 represents that portion of total fatty acyl lipid intensity due to linoleic plus linolenic expected to appear at 2.50–2.84 ppm (and thus overlap with acid resonances); 0.038 represents that portion of total fatty acyl lipid intensity due to linoleic plus linolenic expected to appear at 5.29–5.31 ppm and thus overlap with sucrose; and f represents the ratio (linoleic plus linolenic intensity)/(total fatty acyl intensity), which is obtained from the published weight ratios of fatty acids in standard spectrum. The total acid integral was calculated as

$$\sum_\delta I_{\text{acid},\delta} = I_{(4.18\text{–}4.44\text{ ppm})} + I_{(2.50\text{–}2.84\text{ ppm})} - 0.019 I_{(0.66\text{–}2.50\text{ ppm})} f \quad (3b)$$

where the first term corresponds to the CH proton of malic acid, the second term corresponds to CH_2 protons of malic and citric acids plus methylene protons at positions between double bonds in polyunsaturated fatty acyl chains of lipids, and the third term corrects for the contribution at 2.50–2.84 ppm due to lipid.

Weight ratios (grams of component per gram of water) were calculated from results of integration as

$$r_{i,w} = w_i/w_w = n_w/I_w M_w \sum_\delta I_{i\delta}(M_i/n_{i\delta}) \approx (n_w/M_w)(M_i/n_i)(\sum_\delta I_{i\delta})/I_w \quad (4)$$

where the summation is over all resonances of component i, corrected as above for overlap, and the summation $(M_i/n_{i\delta})$ has been approximated by (M_i/n_i). Here w is the weight of component i in the sample contained within the receiver coil, $I_{i,\delta}$ is the integral over the chemical shift range δ of the resonance assigned to component i, M_i is molecular weight, and $n_{i,\delta}$ is the number of hydrogen nuclei of component i contributing to the integral over δ.

Concentration of a particular component as percent of fresh weight was calculated from the weight ratio $r_{i,w}$ as

$$c_i = r_{i,w} f_w \quad (5)$$

where f_w is the measured water content [(grams of water per 100 g of sample) ×%]. The spectral regions chosen for integration are indicated in the legend to Figure 4.

RESULTS AND DISCUSSION

Field Dependence of Line Widths in Conventional Spectra. The results of applying the single-pulse sequence to grape, banana, and apple tissue samples in a conventional high-resolution probe in a 4.7-T (200 MHz ^1H) spectrometer are shown in the spectra of Figure 1. In these spectra, the water resonance, assigned to 4.76 ppm, strongly dominates. The line widths of the water resonance for grape, banana, and apple are 18.4, 70.9, and 75.9 Hz, respectively. In contrast, the corresponding water line widths observed under similar conditions in homogeneous solutions of pure glucose are 14 and 27 Hz at 10 and 20 wt %, respectively. This range in concentration corresponds to the range in total sugar concentration in ripe fruits. Evidently, water in grape does not experience much line broadening. The difference between fruit and pure solution line widths, up to 49 Hz, suggests a sample-dependent line-broadening mechanism for water.

The sugar resonance widths in fruit must be greater than the separations between peaks, since only a broad sugar envelope centered at about 3.6 ppm can be seen. The sugar resonance widths for fruits in the conventional probe are also sample dependent (grape < apple, banana), ranging from about 0.05 to 0.25 ppm, or from 10 to 50 Hz. In contrast, the corresponding nonexchangeable proton line widths in glucose solution range from 3.17 to 3.57 Hz for solutions at 10 and 20 wt %, respectively. Thus, the sample-dependent line broadening of sugar resonances in fruit can be up to 46 Hz, a value that is similar to the water resonance broadening. This suggests a similar mechanism

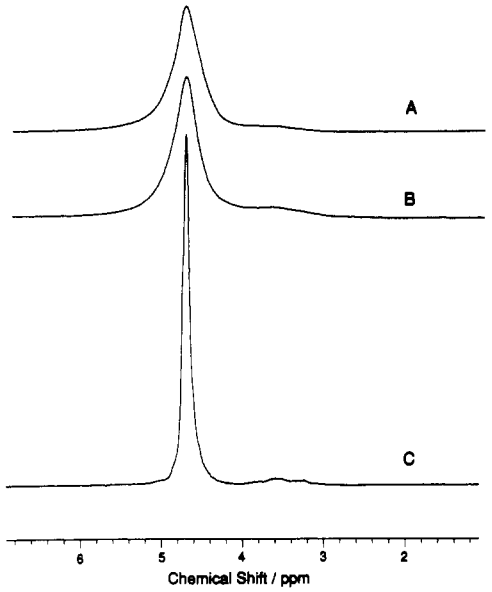

Figure 1. Conventional single-pulse high-resolution ^1H NMR spectra (200 MHz) of intact fruit tissues using a long cylindrical sample in a tube parallel to the magnetic field, no spinning: (A) apple; (B) banana; (C) grape. Vertical scaling is the same for each spectrum. Four scans were obtained.

for excess broadening. Even the broadened lines have widths that are very narrow compared with solids and could still correspond to rapid rotational motional averaging of the strong local magnetic interactions (dipolar and chemical shift anisotropy) likely to dominate in water and carbohydrates. Since it is not known *a priori* whether motional narrowing is less efficient in fresh fruit than in pure solution, it is necessary to measure molecular motion experimentally (see below).

The broadening can be explained by sample susceptibility effects (Doskocilova et al., 1975) as follows. Fruit is an inhomogeneous material, since it contains vacuoles and granules of various kinds, cell walls, air voids, etc. These different physical domains have different bulk magnetic susceptibilities and are thus magnetized to different extents when immersed in the strong magnetic field. The magnetized domains then produce position-dependent magnetic field variations in the space around them. Thus, for each NMR-observable species, there is a spread in resonance frequencies. The observed resonance is then said to be inhomogeneously broadened. For the simplest case of a thin liquid shell surrounding a spherical particle, the susceptibility broadening is approximated by

$$\Delta\nu_\chi = (8\pi/3)\gamma B_0 \Delta\chi \qquad (6)$$

where $\Delta\chi$ is the difference in bulk magnetic susceptibilities (dimensionless) of particle and liquid, γ is the gyromagnetic ratio (hertz/tesla) for the observed nucleus, and B_0 is the magnetic field strength (tesla). Less broadening than this would be observed when not all of the liquid is contained in a thin shell. A more complete analysis indicates the importance of liquid diffusion rate and size of particles (Doskocilova et al., 1975).

The theory suggests that materials with greater microstructural heterogeneity will show greater broadening. The observed order of broadening (apple, banana > grape) (Figure 1) is consistent with this suggestion. This is the same order as previously observed in the ^{13}C NMR study (Ni and Eads, 1992a). Also, since $\gamma_H/\gamma_C \approx 4$, non-MAS ^1H line widths for sugars are expected and observed to be about 4 times larger than ^{13}C line widths measured at the same magnetic field strength.

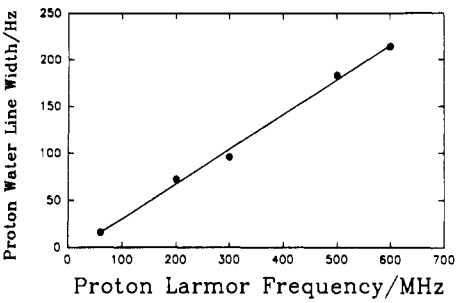

Figure 2. Field strength dependence of water proton line width in ^1H NMR spectra obtained without magic angle spinning. Cylindrical samples were contained in a tube either parallel (14.1-, 11.75-, 7.05-, 4.7-T superconducting solenoid magnets) or perpendicular (1.41-T permanent magnet) to the static magnetic field. Corresponding ^1H resonance frequencies are 600, 500, 300, 200, and 60 MHz. Pulse Fourier transform (superconducting magnets) or frequency sweep continuous wave experiments were executed. The full width at half-height is plotted.

Susceptibility broadening should be linearly proportional to field strength. The value of $\Delta\nu_\chi$ can be estimated experimentally as the difference between the observed widths obtained without and with MAS. Since it was not possible to obtain MAS line widths at all fields, and since $\Delta\nu_\chi$ was found to dominate line width at higher fields, the plot of observed line width $\Delta\nu_{1/2}$ (full width at half-height) rather than broadening was made. The water line width for banana tissue is observed to be linear over the B_0 range 1.41–14.1 T (60–600 MHz ^1H) (Figure 2). The slope of the line at higher fields can be taken as a measure of the susceptibility effect, reflecting both geometry (microstructure) and susceptibility differences (composition of phases). The slope for water in ripe banana is 15.7 Hz/T. Since not all components experience the same environment, the slope for other components could be different.

Resolution Improvement by Magic Angle Spinning. According to theory and experiment, MAS can reduce inhomogeneous broadening in general (Lowe 1959; Andrew, 1971) and susceptibility broadening of liquids in particular (Doskocilova and Schneider, 1970; Doskocilova et al., 1975). Figure 3 compares banana spectra obtained in a conventional high-resolution probe (sample axis parallel to B_0, nonspinning) (Figure 3A) with those obtained with MAS (Figure 3B–D). A great improvement in resolution has been achieved. Similar improvements were obtained with grape and apple tissue (Figure 4), uncovering the differences among fruits due to different solute compositions. The MAS line widths of water and sugar resonances did not deviate much among the fruits tested. The widths of the water proton resonances were between 8 and 10 Hz, while those for sugars were estimated to be 5–6 Hz. These values are still larger by 2–3 Hz than those obtained on solutions of the pure sugars. This is further discussed under Optimizing Resolution.

MAS at rates comparable to the broadening ($\nu_r \sim \Delta\nu_\chi \sim 50$ Hz) would have produced significant spinning side band (SSB) intensity with spacings equal to the spinning frequency. At the frequency used for spectra in Figures 3 and 4 ($\nu_r \approx 1000$ Hz $\gg \Delta\nu_\chi$) SSB intensity is measurable but negligible ($\sim 10^{-3}$ of sugar intensity) and appears outside the regions plotted.

The line width reduction, improved resolution, and improved S/N are consistent with those obtained using MAS ^{13}C NMR on similar samples in the same spectrometer (Ni and Eads, 1992a).

Water Peak Suppression and Dynamic Range Enhancement. Total sugars constitute 15–20% of the fresh weight of ripe banana (Loesecke, 1950; Palmer, 1971)

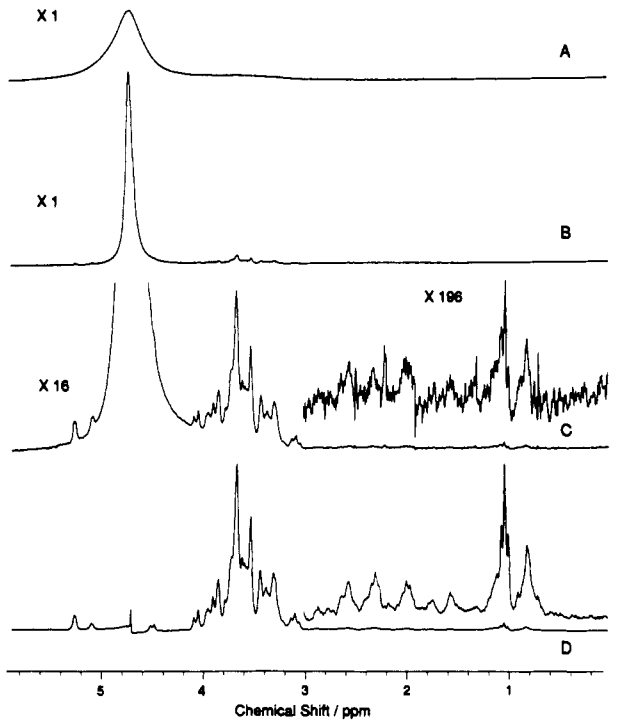

Figure 3. ^{1}H NMR spectrum (200 MHz) of intact banana fruit tissue: (A) non-MAS spectrum obtained in a conventional high-resolution probe with sample axis parallel to magnetic field; (B) MAS spectrum obtained without water peak suppression; (C) vertical expansion of (B); (D) MAS spectrum obtained with water peak suppression. The signal-to-noise ratios in spectra C and D are 55 and 1137, respectively. MAS rate was 1.05 kHz.

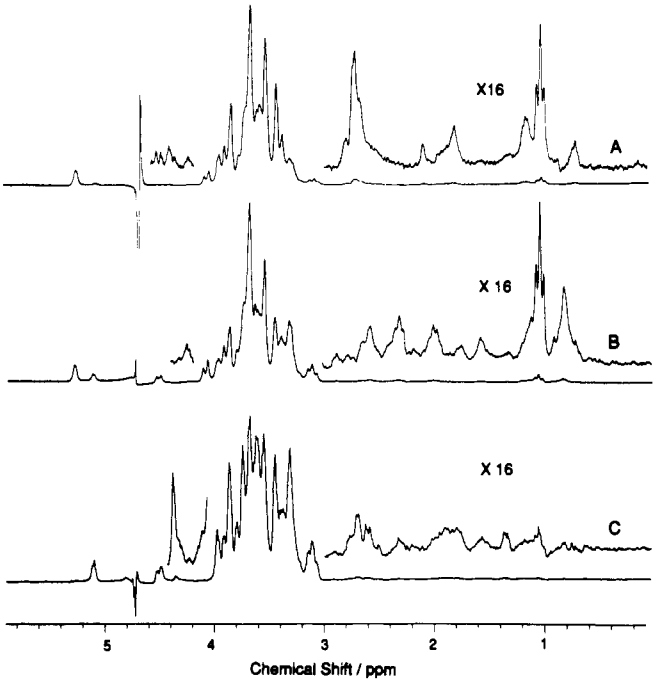

Figure 4. ^{1}H NMR spectra (200 MHz) of different fruit tissues obtained with MAS and water peak suppression: (A) apple (4 scans); (B) banana (4 scans); (C) grape (16 scans). Vertical scaling is adjusted for convenient display. Chemical shift assignments for apple (A) are as follows: 0.72–1.00 ppm, lipid methyl (CH_3); 1.00–2.49 ppm, lipid methylene (CH_2); 2.49–2.98 ppm, malic or citric acid and possibly overlapping lipid methylene; 3.14 ppm, Glu H-2; 3.20–3.83 ppm, combined Glu, Fru, and Suc ring protons; 3.89–4.01 ppm, combined Fru and Suc ring protons; 4.12 ppm, Suc H-3′; 4.21–4.33 ppm, malic acid; 4.33–4.49 ppm, quinic acid; 4.54 ppm, β-Glu H-1; 5.13 ppm, α-Glu H-1; 5.30 ppm, Suc H-1 and CH protons (unsaturation) in fatty acyl chains of lipids. The assignments for banana (B) are as follows: 0.68–1.00 ppm, lipid methyl (CH_3); 1.00–2.52 ppm, lipid methylene (CH_2); 2.52–2.98 ppm, malic or citric acid and possibly overlapping lipid methylene; 3.14 ppm, Glu H-2; 3.20–3.83 ppm, combined Glu, Fru, and Suc ring protons; 3.89–4.01 ppm, combined Fru and Suc ring protons; 4.12 ppm, Suc H-3′; 4.21–4.33 ppm, malic acid; 4.54 ppm, β-Glu H-1; 5.13 ppm, α-Glu H-1; 5.30 ppm, Suc H-1 and CH protons (unsaturation) in fatty acyl chains of lipids. The assignments for grape (C) are as follows: 0.70–1.00 ppm, lipid methyl (CH_3); 1.00–2.49 ppm, lipid methylene (CH_2); 2.49–2.98 ppm, malic or citric acid and possibly overlapping lipid methylene; 3.14 ppm, Glu H-2; 3.20–3.83 ppm, combined Glu, Fru, and Suc ring protons; 3.89–4.01 ppm, combined Fru and Suc ring protons; 4.12 ppm, Suc H-3′; 4.21–4.28 ppm, malic acid; 4.28–4.44 ppm, tartaric acid; 4.54 ppm, β-Glu H-1; 5.13 ppm, α-Glu H-1; 5.30 ppm, Suc H-1 and CH protons (unsaturated) fatty acyl chains of lipids.

and are easily observed in a simple MAS experiment (Figure 3B). However, upon water peak suppression by presaturation, further improvement in S/N is achieved (compare vertical expansions of Figure 3C,D), and resonances from components present at levels in the 0.01–0.5% range, namely fatty acyl lipids and organic acids, become detectable even in only four scans. These results might be achievable without suppression by increasing the number of bits of digital "resolution" in the analog-to-digital converter. However, without suppression, peaks on the shoulders of the water resonance would remain unobservable or severely distorted. While sugars were observable in ^{13}C MAS NMR spectra of ripe fruit tissues (Ni and Eads, 1992a), the organic acids and lipids were not, at least with the single-pulse method used.

Resonance Assignments and Qualitative Analysis. Chemical shift assignments for all three fruits are given in Figure 4. Assignments were made on the basis of published results for glucose, fructose, sucrose, fatty acids, malic acid, citric acid, and tartaric acid. Assignments were sometimes verified by comparison with spectra of solutions of various components (not shown).

Resonances unique to various components can be readily identified. For sugars, the resolved triplet at 3.14 ppm is due to β-Glu H-2; the resolved doublet at 4.54 ppm is due to β-Glu H-1; an unresolved doublet at 5.12 ppm is due to α-Glu H-1; the resolved doublet at 4.12 ppm is due to Suc H-3′; and the unresolved doublet at 5.31 ppm is due to Suc H-1. The resonances at 3.89, 3.94, and 3.99 ppm are due to the overlapping resonances of ring protons of fructose and sucrose. For acids, the unresolved triplet at 4.26 ppm is due to the CH proton of malic acid (the CH_2 protons of malic overlap with lipid methylene); the unresolved doublet at 4.39 ppm is due to the two CH protons of tartaric acid. For lipids, the methyl protons resonate near 0.9 ppm, and a principal methylene peak is always present at 1.2 ppm.

In contrast to results obtained with ^{13}C NMR (Ni and Eads, 1992a), there are fewer ^{1}H resolved resonances from sugars. This is mainly due to the 20-fold smaller range in chemical shifts for ^{1}H. This is further discussed below.

Lipids constitute about 0.3% of the fresh weight of ripe banana pulp (Goldstein and Wick, 1969; Palmer, 1971). About one-third of the lipid is comprised of fatty acyl groups. Among these, palmitic, stearic, oleic, linoleic, and linolenic acids dominate (Goldstein and Wick, 1969). In Figure 3D these appear to be represented by methyl (CH_3) resonances from 0.75 to 1.0 ppm and by methylene (CH_2) resonances of various types from 1.0 to 2.8 ppm. Methene (CH) resonances expected in the 5.3 ppm region may overlap with sucrose H-1. The appearance of narrow aliphatic resonances can indicate either that the molecules are in a liquid-like state, such as triacylglycerol molecules in oil droplets, or that residual static dipolar interactions

Table I. Quantitative Analysis of High-Resolution ^1H NMR Spectra of Various Fruit Tissues

	NMR intensity[a] (%)				weight ratios[b] (g of component/100 g of H_2O)			composition (g of component/100 g of sample) × 100%			
sample	water	sugars	acids	lipids	sugars	acids	lipids	water[c]	sugar	acids	lipids
apple	93.96	5.81	0.11	0.12	10.30	0.30	0.12	85.01	8.24	0.26	0.10
banana	85.82	13.50	0.24	0.44	26.24	0.70	0.45	75.71	19.86	0.53	0.34
grape	92.97	6.87	0.08	0.08	12.31	0.21	0.08	81.49	10.14	0.17	0.06

[a] Single determination on samples represented in the spectra of Figure 4. Spectral regions of integration are indicated in Figure 4. [b] Calculated as described under Experimental Procedures. [c] Values obtained by oven-drying method. [d] Calculated as described under Experimental Procedures, on the basis of measured water contents.

Table II. Sugar Composition of Single Samples of Intact Tissues of Various Fruits Determined by High-Resolution ^1H NMR

	sugar composition[a] (g/100 g of sample) × 100%							
fruit	total	lit.	sucrose	lit.	glucose	lit.	fructose	lit.
apple	8.24	10.99[b]	3.91	3.78[b]	0.47	1.17[b]	3.84	6.04[b]
banana	19.86	19.60[c]	9.90	8.50[c]	4.23	5.20[c]	5.73	5.90[c]
grape	10.14	9.30[c]	0.29	0.20[c]	3.65	4.30[c]	6.20	4.80[c]

[a] Single determinations; determined by simulation (see eq 7 in text) based on standard 20 wt % glucose, sucrose, and fructose solution ^1H NMR spectra. [b] Ockerman (1991). [c] Ensminger and Ensminger (1983).

in the liquid crystalline state have been removed by MAS, as for acyl chains of phospholipids in membranes [e.g., Forbes et al. (1988)]. Similar considerations apply to the lipids in apple and grape.

Total organic acidity in ripe banana pulp is about 11 mequiv/100 g of fresh weight (Palmer, 1971; Wyman and Palmer, 1964); in apple, it is also about 11 mequiv (Hulme and Rhodes, 1971); and in grape up to 90 mequiv (Peynaud and Ribereau-Gayon, 1971). In each fruit, there are several acids. The major organic acids include malic, with resonances expected to appear at about 2.67 and 4.35 ppm, citric, expected to appear at 2.68 ppm, oxalic, expected to appear at 2.59 and 3.31 ppm, and tartaric, expected to appear at 4.39 ppm. Most of these were directly observed in fruit spectra (Figure 4).

The differences in sugar, lipid, and acid composition among samples are obvious by inspection of the spectra in Figure 4, and this was verified by quantitative analysis.

Quantitative Analysis. A quantitative analysis of sugars, acids, and lipids may be made by ^1H NMR. Since the NMR signal is proportional to the number of nuclei of each chemical type, integrals can be converted to molar fractions. If the content of any component is known by an independent measurement (water, for example), then molar fractions can be converted to percent of fresh weight (see Experimental Procedures). Table I contains the results of such an analysis for single samples of grape, banana, and apple tissue.

We wish to emphasize that these results were obtained without disruption of tissue beyond cutting a cylindrical piece; that no separation of components by physical or chemical means was required; no chemical modifications were required; no spectroscopic methods other than NMR were needed to identify components; and that the numbers were obtained without recourse to calibration of NMR signals with external standards.

The values for sugars are in fair agreement with averages reported in standard references (see legend to Table I). The values reported are for single pieces of fruit, and so uncertainties are not reported here. However, the uncertainty in a single NMR measurement depends primarily on the S/N of the observed resonances and on the quality of the baseline in the vicinity of the resonance. Thus, relative uncertainties of individual NMR intensities are smaller for sugars (about 0.02%) and probably larger for acids and lipids (about 0.05%). Further work would be required to explore the sources of variance in NMR measurements. For example, we have observed qualitative and quantitative differences in experiments on other samples of apple, banana, and grape tissue. These differences very likely include the influences of cultivar, growth, time of harvest, conditions of storage, and treatments used to inhibit or stimulate ripening. Further work would also be required to further explore the accuracy of the method. Accuracy would be partly established by running parallel, independent analysis of chemical composition using standard methods. Accuracy of the NMR method itself would be improved by employing chemometric methods for spectral data analysis.

Amounts of individual sugars (sucrose, glucose, and fructose) were estimated as follows. Spectra of standard solutions of sugars in water were added in various proportions until the intensity and shape of the observed sugar region of the spectrum of a particular fruit were reproduced. This procedure is represented by the formula

$$I = a_s I_s + a_f I_f + a_g I_g \qquad (7)$$

where I is the simulated spectrum, I_i are the standard spectra, and a_i are the relative fractions of sugars. The usual requirements for quantitative NMR have been met (Rabenstein and Keire, 1991; Martin et al., 1980). The results, presented in Table II, illustrate the detailed information which can be extracted from NMR spectra. The values compare fairly well with those in standard references and to previous results of carbon-13 NMR analysis (Ni and Eads, 1992a). The NMR method is obviously well suited for nondestructive analysis of both total sugar and sugar composition.

^1H Longitudinal Relaxation (T_1) and Rotational Mobility of Sugars Measured *in Situ*. Nuclear relaxation has practical implications for analytical sensitivity. Also, relaxation measurements can be used to quantify molecular translation and reorientation. Finally, differential relaxation is also a basis for contrast in magnetic resonance imaging. Thus, measurement of the ^1H longitudinal relaxation times T_1 of the nonexchangeable ring protons of glucose, fructose, and sucrose in banana, and in solutions of the individual sugars, was undertaken. The inversion–recovery Fourier transform method (IRFT) with MAS at 450 Hz was used. Water peak suppression was not employed. The particular resonances chosen are the triplet centered at 3.14 ppm corresponding to the Glu H-2 proton and the doublet centered at 4.12 ppm corresponding to the Suc H-3′ proton. For the case of fructose, which does not present unique resonances in banana, T_1 was obtained by fitting intensities of the peak at 3.89 ppm, which is dominated by sucrose and fructose, as described under Experimental Procedures. The T_1 of water proton was also measured and tabulated. The results are presented in Table III. T_1 values for glucose, fructose, and sucrose in banana are similar to those of the individual pure sugars in 20% aqueous solutions.

The T_1 values of sugars in banana are fairly long. This places a limit on S/N achievable during signal averaging, since relaxation must be permitted to occur between successive shots. Pulse methods to optimize S/N require prior knowledge of the longest analyte T_1 (Martin et al., 1980). The longest T_1 in the fruit is that of water, but since the water peak is usually suppressed, the longest T_1 of the sugars is that of glucose (Table III).

Although our single-frequency single-temperature measurement does not indicate on which side of the T_1 minimum the values lie, previous determination of ^{13}C T_1 values and NOEs established that molecular motion of glucose in banana is in the extreme narrowing regime, defined as $\omega\tau_r \ll 1$, where ω is the resonance frequency in radians per second and τ_r is the rotational correlation time in seconds.

It is important to try to understand the meaning of the observed T_1 values by attempting to rationalize them in terms of relaxation processes. As will be shown, this also provides insight about rotational motion and local viscosity. The calculation was performed for glucose as follows. Since only nonexchangeable protons were observed, proton-exchange contributions are irrelevant. Thus, the overall relaxation rate may be written as a sum of intramolecular and intermolecular nuclear dipole–dipole (DD), chemical shift anisotropy (CSA), and paramagnetic (P) terms:

$$1/T_1^{\text{overall}} = 1/T_1^{\text{DD,intra}} + 1/T_1^{\text{DD,inter}} + 1/T_1^{\text{CSA}} + 1/T_1^{\text{P}} \quad (8)$$

These may be calculated from the usual formulas [see, for example, Sudmeier et al. (1990)] that assume that molecular motion is in the extreme narrowing range. An estimate shows immediately that $1/T_1^{\text{CSA}}$ is smaller compared to the other terms (less than 8×10^{-4} s^{-1}). While $1/T_1^{\text{P}}$ may, in principle, be calculated (Sudmeier et al., 1990), there is not enough information to do so in the present case, since the concentrations of the probable paramagnetic species [dissolved singlet oxygen (O_2) and manganese ion] are not known. Instead, this term was estimated for glucose solution as the difference between the rates obtained with air-saturated and degassed samples. The samples were made with distilled, filtered, deionized water (16 Megohm cm). The difference was 0.1 s^{-1}, which is taken as an estimate for $1/T_1^{\text{P}}$.

The remaining terms are calculated from the expressions

$$1/T_1^{\text{DD,intra}} = (^1/_2\pi)^2\gamma_H{}^4h^2I(I+1)\sum r_i^{-6}\tau_r \quad (9)$$

$$1/T_1^{\text{DD,inter}} = (^2/_3kT)\gamma_H{}^4h^2\eta N_0 \quad (10)$$

where γ_H is the gyromagnetic ratio for proton, I is the spin quantum number ($I = {}^1/_2$ for ^1H), r_i is a distance between protons in the same molecule, k is the Boltzmann constant, h is Planck's constant, T is the absolute temperature, η is the solution viscosity, and N_0 is the number of protons per cubic centimeter in the solution. The expression for $1/T_1^{\text{DD,intra}}$ accounts for the fact that several interproton distances are found in a single molecule. The expression for $1/T_1^{\text{DD,inter}}$ includes both solvent–solute and solute–solute magnetic interactions and assumes that fluctuations in the local dipolar field are driven by translational motion.

For calculation, the constants are known (k, T, h, γ_H) and parameters must be estimated (η, Σr_i^{-6}, N_0, τ_r, and $1/T_1^{\text{P}}$). Viscosity measurements were made in an Ostwald viscometer at 22 °C and yielded $\eta = 0.0183$ P for 20 wt % glucose in water (H_2O). The interproton distance r is 1.58 $\times 10^{-8}$ cm for water (Abragram, 1983). For calculation of Σr_i^{-6}, only distances between protons separated by four bonds or fewer were considered, on the basis of a molecular model of glucose. For the distances from β-Glu H-2 the value 2.22×10^{48} cm^{-6} was calculated for Σr_i^{-6}. The value of N_0, 6.27×10^{22} spins/cm^3, was calculated from the measured solution density, which was 1.09 g/cm^3. For τ_r the value used was 64×10^{-11} s for glucose, as measured in the previous ^{13}C NMR study (Ni and Eads, 1992a).

Table III. ^1H Longitudinal Relaxation Times T_1 of Sugars in Banana and in Solution

component	resonance (chemical shift in ppm)	T_1[a] (s) sugar in H_2O	sugar in banana[b]	sugar in D_2O
glucose	3.14	0.69[c]	0.68	1.41[c]
fructose	3.89	0.57[c]	0.49[d]	–[f]
sucrose	4.10	0.48[c]	0.43	–[f]
^1H_2O	4.76	1.88[e]	1.38	–[f]

[a] IRFT method with magic angle spinning; temperature = 22 ± 1 °C (see Experimental Procedures for details). [b] Edible portion of ripe fruit. [c] 20 wt % solution; not degassed. [d] T_1 obtained from analysis of overlapping sucrose and fructose resonances (see Experimental Procedures). [e] T_1 of ^1H_2O in 20 wt % glucose solution in water. [f] Not determined.

Substituting these values into the expressions, we obtain for 20 wt % glucose at room temperature $1/T_1^{\text{DD,intra}} = 0.59$ s^{-1} and $1/T_1^{\text{DD,inter}} = 0.42$ s^{-1}. Since the interproton distances in sugar molecules are relatively large, inter- and intramolecular contributions of the same order were anticipated. As a check on the value of $1/T_1^{\text{DD,intra}}$, relaxation of glucose nonexchangeable protons in a sample of 20 wt % glucose in D_2O (not degassed) was measured. In this solution the intermolecular interaction is reduced to a minimum, and the intramolecular and paramagnetic contributions should dominate. The result is $T_1^{\text{DD,intra+P}} = 1.41$ s, or $1/T_1^{\text{DD,intra+P}} = 0.71$ s^{-1}, which is in fair agreement with the calculated value of $1/T_1^{\text{DD,intra}} + 1/T_1^{\text{P}} = (0.59 + 0.1)$ s^{-1} = 0.69 s^{-1}, or $T_1^{\text{DD,intra+P}} = 1.46$ s. The overall rate is then $(0.59 + 0.42 + 0.1)$ s^{-1} = 1.11 s^{-1}, or $T_1^{\text{overall}} = 0.90$ s. This compares well with the experimental value $1/T_1^{\text{obs}} = 1.45$ s^{-1} or $T_1^{\text{obs}} = 0.69$ s. The difference is small for this kind of calculation. It is plausible that, in the natural material, there might be a stronger paramagnetic contribution than in the nondegassed solution of glucose and that this could partially account for the observed difference. Nonetheless, the substantial agreement suggests that rotational and translational motions provide the fluctuations in magnetic dipolar fields needed to drive longitudinal relaxation.

The above calculation does not take into account the possibility that sugars might participate in diffusive exchange between regions of space in which longitudinal relaxation or resonance frequency is different. There is no evidence at this time that such an exchange needs to be considered.

It would be convenient if measurements of longitudinal relaxation rate could be used as an index of the local viscosity experienced by solutes as they occur in cells and interstitial space. Viscosity does not affect the paramagnetic term; it appears directly in the intermolecular term, and it appears indirectly in the intramolecular term through τ_r, whose hydrodynamic meaning is given by the Stokes–Einstein relation $\tau_r = 4\pi\eta a^3/3kT$, where a is the radius of the equivalent hydrodynamic sphere. Thus, it is conceivable that viscosity could be obtained in a parametric fit of observed relaxation rate to eqs 9 and 10. Experimental studies on model systems would be required to ascertain whether $1/T_1^{\text{obs}}$ of particular solutes would

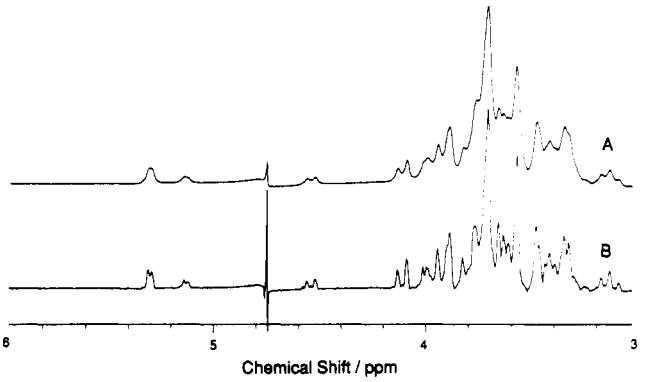

Figure 5. Improvement of spectral resolution in banana by using a combined Gaussian–exponential multiplication of the free induction decay (see text for details): (A) standard spectrum (exponential multiplication applied to improve apparent signal-to-noise ratio, equivalent to +1-Hz line broadening); (B) resolution-enhanced spectrum (Gaussian multiplication equivalent to +2-Hz line broadening and exponential multiplication equivalent to −3-Hz line narrowing).

provide a fair index of viscosity. To the extent longitudinal relaxation can be shown to reflect local molecular dynamics, it could be used to study molecular events accompanying physical change during processes such as freezing and dehydration.

Optimizing Resolution. MAS greatly improved resolution in fruit spectra. In fact, sugar line widths estimated for fruit (e.g., 5.8 Hz for the central peak of the resolved triplet of β-glucose H-2 at 3.14 ppm) were only about 1 Hz larger those estimated from the solution spectrum (e.g., 4.9 Hz for glucose at 20 wt %) obtained in the MAS probe. However, the absolute value for glucose solution in the MAS probe is 2.7 Hz larger than the value in the conventional probe, which itself includes 0.3-Hz broadening. Thus, instrumental broadening contributes about 3.0 Hz to observed line widths in all spectra obtained in the MAS probe. This probably obscures the resolution truly achievable with MAS and also obscures the true line width. The true width would be compared to the width calculated from direct measurements of T_1 and T_2 to understand molecular motions and interactions *in situ*.

A data manipulation method such as Gaussian–exponential multiplication function applied to a FID can improve the apparent resolution (Figure 5). Here the line width of Suc H-3′ at 4.12 ppm in the banana spectrum is reduced from 6 to 4 Hz, with an obvious improvement in overall appearance. Peaks are revealed that were not evident without the data manipulation. Thus, resolution enhancement is a valuable addition for qualitative analysis. However, it is important to consider how to optimize resolution without data manipulation.

Resolution is defined as the ability to distinguish neighboring resonances; that is, the line width of each resonance must be less than the separation between their isotropic chemical shifts. To achieve this, instrumental factors must first be optimized. This includes a well-designed probe, good shimming, a strong stable magnetic field, accurate setting of the magic angle, stable spinning speed, good temperature control (since chemical shifts are temperature dependent), and uniform temperature throughout the sample. The instrumental broadening that results from all of the above factors will exceed the line width due to nuclear relaxation. Susceptibility inhomogeneity adds more width but is supposed to be eliminated by MAS if the spinning rate is much greater than the maximum susceptibility broadening (eq 6; Doskocilova et al., 1975).

Directly measured transverse relaxation of liquid-phase components would provide a critically important probe of diffusive and exchange processes occurring *in situ*. Such dynamical processes are likely to be important in higher order processes such as drying, crystallization, texture development, and flavor release. Such measurements are also required to estimate the relaxation contribution to line width, so that the maximum resolution so deduced can be set as a target for analytical instrument development. While transverse relaxation results for nonexchangeable proton on specific solutes are not reported here, the measurements are made possible for the first time by the achievement of high resolution.

While resolution is better at higher fields due to the chemical shift effect, high-resolution spectroscopy is still possible at lower fields (e.g., 1.5 T), as long as the field can be made homogeneous to about 1 part in 10 million over the dimensions of the sample active in the NMR experiment, and as long as the other criteria for instrumental performance are met. What then can be expected in NMR of heterogeneous materials at lower fields? It is speculated that nonspinning spectra would be similar at high and low fields. Rationale for that is that the susceptibility effect (broadening) decreases with field and chemical shift effect (peak separation) also decreases. With MAS, the peak separation advantage of higher field would be retained, if line widths are dominated by dipolar effects, which do not depend on field. While resolution might be inferior at lower fields, only experimentation would reveal how much analytically useful information is retained in the high-resolution lower field MAS experiment.

Potential Applications. The *in situ* study of components in agricultural materials and food by NMR is a growing field. Studies have been reported for water (Schmidt et al., 1990), metal ions (Belton et al., 1985; Schmidt et al., 1990; Pfeffer et al., 1990), liquid-phase small organic molecules (Rutar, 1989; Ni and Eads, 1992a; Martin et al., 1985), and semisolid and solid-phase components (Halladay et al., 1990; Maciel et al., 1985; Belton et al., 1988; Baianu et al., 1990; Eads, 1991, 1992; Ni and Eads, 1993). The high-resolution ^{1}H methods have particular value for liquid-phase organic components since ^{1}H is an abundant and sensitive nucleus. MAS, shown to be useful in observation of ^{1}H and ^{13}C, should also apply to ^{31}P and other nuclei whose liquid resonance widths may be inhomogeneously broadened.

The current work demonstrates the potential of ^{1}H MAS NMR for specific analyte quantitation. However, the spectrum may also be regarded as a pattern. Pattern recognition and principal component analysis would be useful for classifying heterogeneous materials on the basis of NMR spectra, even if they are not fully resolved, e.g., for identifying sources of raw materials or for identifying instances of adulteration. Spectral simulation and target component analysis would be useful for extracting more detailed chemical information. These are all subject to automation, as are the NMR measurements themselves, and could be implemented in computerized analytical devices. Maximizing information content and minimizing ambiguity of resonance assignments is one goal of multidimensional NMR, which was demonstrated in the ^{1}H homonuclear correlation (COSY) spectrum of intact grape tissue (Ni and Eads, 1992b).

With the advent of compact high-resolution NMR spectrometers for analysis and process sensing, methods such as MAS, or its equivalent in resolution improvement, may become important in food ingredient assessment, analysis of intermediates, quality assessment, readiness

for eating, analysis of agronomic materials, commodity value based on level of most valuable component, etc. The chemical information obtained, and physical information obtainable on the same sample using solids-selective proton methods such as cross relaxation NMR (Wu and Eads, 1992, 1993), could also be used in computer-integrated manufacturing. Significant advances in this area have already been made (Guillou and Tellier, 1988).

Scientific applications in agriculture include rapid, nondestructive analysis of liquid-phase components in complex materials as affected by phenotype, stage of growth, growth conditions, postharvest treatment, etc. Some possible materials for study include fermenting biomass, fresh vegetables, fruit, meat, soils, grains, plant stems and leaves, and many others. The high-resolution NMR method has been applied to chemical change during ripening of bananas (Ni and Eads, 1993).

Conclusion. Reduction of susceptibility broadening in ^{1}H NMR spectra of intact tissues by MAS has the following advantages: (1) Resolution and thus selectivity are increased, permitting simultaneous observation of several sugars, acids, and lipid species, even when these occur in separate phases. (2) The signal-to-noise ratio of analyte peaks is increased. (3) Integrals of solute resonances are proportional to molar composition and can be converted to convenient units such as percent of sample weight. (4) It becomes possible to apply saturation or other solvent suppression methods. (5) ^{1}H nuclear relaxation can be measured for specific liquid-phase components, enabling analysis of molecular motions and interactions of selected components. (6) By applying water peak suppression, dynamic range is increased for detection of solutes present at levels as low as 0.01 wt %. The lower limit of sensitivity has not been reached in the experiments reported. Further reductions in instrumental broadening are conceivable. The limits of selectivity have not yet been fully explored either spectroscopically or instrumentally. The methods described here are straightforward and general; they should be adaptable for benchtop NMR chemical analyzers and can be applied to other multiphasic agricultural, food, and nonbiological materials.

ACKNOWLEDGMENT

This is Paper 13698 from the Indiana Agricultural Experiment Station, West Lafayette, IN. We gratefully acknowledge financial assistance from the sustaining members of the Whistler Center for Carbohydrate Research, Purdue University, and from Nestec Ltd., Lausanne, Switzerland. We thank J. Lowens and J. M. Ariano of Great Lakes Chemical Corp., West Lafayette, IN, for providing low-field non-MAS spectra.

LITERATURE CITED

Abragram, A. *The Principle of Nuclear Magnetism*; Oxford University Press: London, 1983; p 327.

Andrew, E. R. The Narrowing of NMR Spectra of Solids by High Speed Specimen Rotation and the Resolution of Chemical Shift and Spin Multiplet Structure for Solids. *Prog. NMR Spectrosc.* **1971**, *8*, 1–39.

Baianu, I. C.; Kumosinski, T. F.; Bechtel, P. J.; Myers-Betts, P. A.; Yakubu, P.; Mora, A. Multinuclear Spin Relaxation and High-Resolution Nuclear Magnetic Resonance Studies of Food Proteins, Agriculturally Important Materials and Related System. *Basic Life Sci.* **1990**, *56*, 361–389.

Bellon, V.; Cho, S. I.; Krutz, G. W.; Davenel, A. Ripeness Sensor Development Based on Nuclear Magnetic Resonance. *Food Control* **1992**, Jan, 45–49.

Belton, P. S.; Ratcliffe, R. G. NMR and Compartmentation in Biological Tissues. *Prog. NMR Spectrosc.* **1985**, *17*, 241–279.

Belton, P. S.; Hills, B. P.; Raimbaud, E. R. The Effects of Morphology and Exchange on Proton N.M.R. Relaxation in Agarose Gels. *Mol. Phys.* **1988**, *63*, 825–842.

Cho, S. I.; Krutz, G. W. Fruit Ripeness Detection by Using NMR. *ASAE Publ.* **1989**, paper 89-6620.

Cho, S. I.; Bellon, V.; Eads, T. M.; Stroshine, R. L.; Krutz, G. W. Sugar Content Measurement in Fruit Tissue Using Water Peak Suppression in High Resolution ^{1}H Magnetic Resonance. *J. Food Sci.* **1991**, *56*, 1091–1094.

Coombe, B. G.; Jones, G. P. Measurement of the Changes in the Composition of Developing Undetached Grape Berries by Using ^{13}C NMR Techniques. *Phytochemistry* **1983**, *22*, 2185–2187.

Doskocilova, D.; Schneider, B. Narrowing of Proton NMR Lines by Magic Angle Rotation. *Chem. Phys. Lett.* **1970**, *6*, 381–384.

Doskocilova, D.; Tao, D. D.; Schneider, B. Effect of Macroscopic Spinning Upon Linewidth of NMR Signals of Liquid in Magnetically Inhomogeneous System. *Czech. J. Phys.* **1975**, *B25*, 202–209.

Eads, T. M. Multinuclear High Resolution and Wide Line NMR Methods for Analysis of Lipids. In *Analyses of Fats, Oils and Lipoproteins*; Perkins, E. G., Ed.; American Oil Chemists' Society: Champaign, IL, 1991; pp 409–457.

Eads, T. M.; Bryant, R. G. High-Resolution Proton NMR Spectroscopy of Milk, Orange Juice, and Apple Juice with Efficient Suppression of the Water Peak. *J. Agric. Food Chem.* **1986**, *34*, 834–837.

Eads, T. M. New Strategies for Measuring Molecular Structure, Dynamics, and Composition of Food Materials by NMR. In *Frontiers in Carbohydrate Research—2*; Chandrasekaran, R., Ed.; Elsevier: New York, 1992; pp 128–140.

Eads, T. M.; Weiler, R. K.; Gaonkar, A. G. Detection of Water in the Internal Aqueous Phase of W/O/W Multiple Emulsions Using Magic Angle Spinning Proton NMR. *J. Colloid Interface Sci.* **1991**, *145*, 266–277.

Ensminger, A. H.; Ensminger, M. E. *Foods and Nutrition Encyclopedia*, 1st ed.; Pegus Press: Clovis, CA, 1983; Vol. I, pp 341–342.

Forbes, J.; Husted, C.; Oldfied, E. High-Field, High Resolution Proton "Magic-Angle" Sample-Spinning Nuclear Magnetic Resonance Spectroscopic Studies of Gel and Liquid Crystalline Lipid Bilayers and the Effects of Cholesterol. *J. Am. Chem. Soc.* **1988**, *110*, 1059–1065.

Gebhardt, S. E.; Cutrufelli, R.; Matthews, R. H. *Composition of Foods*; Agriculture Handbook 8-9; USDA Human Nutrition Information Service: Washington, DC, 1982; pp 24, 60, and 135–136.

Goldstein, J. L.; Wick, E. L. Lipid in Ripening Banana Fruit. *J. Food Sci.* **1969**, *344*, 482–484.

Guillou, M.; Tellier, C. Determination of Ethanol in Alcoholic Beverages by Low-Resolution Pulsed Nuclear Magnetic Resonance. *Anal. Chem.* **1988**, *60*, 2182–2185.

Halladay, H. N.; Stark, R. E.; Ali, S.; Bittman, R. Magic Angle Spinning NMR Studies of Molecular Organization in Multibilayers Formed by 1-Octadecanoyl-2-Decanoyl-*sn*-Glycero-3-Phosphocholine. *Biophys. J.* **1990**, *58*, 1449–1461.

Hulme, A. C.; Rhodes, M. J. C. Pome Fruits. In *The Biochemistry of Fruits and Their Products*; Hulme, A. C., Ed.; Academic Press: London, 1971; Vol. 2.

Loesecke, H. W. *Bananas*; Interscience: New York, 1950; Chapter 4.

Longo, P. A.; Tihal, C. A.; Li, Ka-Loh; Stark, Ruth E. High Resolution and Magic Angle Spinning Two-Dimensional NMR Studies of Molecular Organization in Model Substrates for Glyceride Digestion. Presented at the 33rd Experimental NMR Conference, 1992; poster WP 180.

Lowe, I. J. Free Induce Decay of Rotating Solids. *Phys. Rev. Lett.* **1959**, *2*, 285–287.

Maciel, G. E.; Haw, J. F.; Smith, D. H.; Gabrielsen, B. C.; Hatfield, G. R. Carbon-13 Nuclear Magnetic Resonance of Herbaceous Plants and Their Components, Using Cross Polarization and Magic-Angle Spinning. *J. Agric. Food Chem.* **1985**, *33*, 185–191.

Martin, F. Monitoring Plant Metabolism by ^{13}C, ^{15}N, and ^{14}N Nuclear Magnetic Resonance Spectroscopy. A Review of the

Applications to Algae, Fungi and Higher Plants. *Physiol. Veg.* **1985**, *23*, 463–490.

Martin, M. L.; Martin, G. L.; Delpuech, J. *Practical NMR Spectroscopy*; Heyden: Philadelphia, 1980; pp 365–376.

Morris, G.; Hall, L. D. Experimental Chemical Shift Correlation Maps from Heteronuclear Two-Dimensional NMR Spectroscopy. 1. Carbon-13 and Proton Chemical Shifts of Raffinose and Its Subunits. *J. Am. Chem. Soc.* **1981**, *103*, 4703–4711.

Ni, Q. W.; Eads, T. M. Low Speed Magic Angle Spinning Carbon-13 NMR of Fruit Tissue. *J. Agric. Food Chem.* **1992a**, *40*, 1507–1513.

Ni, Q. W., Eads, T. M. High Resolution ^{13}C and ^{1}H Spectroscopy of Liquid Phase Components in Intact Fruit Tissue. Presented at the 33rd Experimental NMR Conference, 1992b; poster MP 154.

Ni, Q. X.; Eads, T. M. Analysis by Proton NMR of Changes in Liquid-Phase and Solid-Phase Components during Ripening of Banana. *J. Agric. Food Chem.* **1993**, following paper in this issue.

Ockerman, H. W. *Food Science Sourcebook*, 2nd ed.; Van Nostrand Reinhold: New York, 1991; Part 2, p 1368.

Palmer, J. K. The Banana. In *The Biochemistry of Fruits and their Products*; Hulme, A. C., Ed.; Academic Press: London, 1971; Vol. 2.

Peynaud, E.; Ribereau-Gayon, P. The Grape. In *the Biochemistry of Fruits and Their Products;* Hulme, A. C., Ed.; Academic Press: London, 1971; Vol. 2.

Pfeffer, P. E.; Rolin, D. B.; Brauer, D. S. I.; Kumosinski, T. F. In vivo ^{133}Cs-NMR a Probe for Studying Subcelluar Compartmentation and Ion Uptake in Maize Root Tissue. *Biochim. Biophys. Acta* **1990**, *1054*, 169–175.

Rabenstein, D. L.; Keire, D. A. Quantiative Chemical Analysis by NMR. In *Modern NMR Techniques and Their Application in Chemistry*; Popov, A. I., Hallenga, K., Ed.; Dekker: New York, 1991.

Rutar, V. Magic Angle Sample Spinning NMR Spectroscopy of Liquids as a Nondestructive Method for Studies of Plant Seeds. *J. Agric. Food Chem.* **1989**, *37*, 67–70.

Rutar, V.; Kovac, M.; Lahajnar, G. Improved NMR Spectra of Liquid Components in Heterogeneous Samples. *J. Magn. Reson.* **1988**, *80*, 133–138.

Schmidt, S. J.; Serianni, A. S.; Finley, J. W. Applications of NMR in Agriculture and Biochemistry. *Basic Life Sci.* **1990**, *56*, 1–6.

Sudmeier, J. L.; Anderson, S. E.; Frye, J. S. Calculation of Nuclear Spin Relaxation Times. *Concepts Magn. Reson.* **1990**, *2*, 197–212.

Tellier, C.; Guillou-Charpin, M.; Grenier, P.; Botlan, D. L. Monitoring Alcoholic Fermentation by Low-Resolution Pulsed Nuclear Magnetic Resonance. *J. Agric. Food Chem.* **1989**, *37*, 988–99.

Vold, R. L.; Waugh, J. S.; Klein, M. P.; Phelps, D. E. Measurement of Spin Relaxation in Complex Systems. *J. Chem. Phys.* **1968**, *48*, 3831–3832.

Wu, J. Y.; Eads, T. M. Evolution of Polymer Mobility during Aging of Gelatinized Waxy Maize Starch: a Magnetization Transfer ^{1}H NMR Study. *Carbohydr. Polym.* **1993**, *20*, 51–60.

Wu, J. Y.; Bryant, R. G.; Eads, T. M. Detection of Solidlike Components in Starch Using Cross-Relaxation and Fourier Transform Wide-Line ^{1}H NMR Methods. *J. Agric. Food Chem.* **1992**, *40*, 449–455.

Wyman, H.; Palmer, J. K. Organic Acids in the Ripening Banana Fruit. *Pl. Physiol. Lancaster* **1964**, *39*, 630.

Received for review January 22, 1993. Accepted April 20, 1993.